ResearchGate

See discussions, stats, and author profiles for this publication at: https://www.researchgate.net/publication/270159324

Origin of the band dispersion in a metal phthalocyanine crystal

Article *in* Physical Review B · December 2014

DOI: 10.1103/PhysRevB.90.245141

CITATIONS
14

READS
386

5 authors, including:

Susumu Yanagisawa
University of the Ryukyus
82 PUBLICATIONS **3,640** CITATIONS
SEE PROFILE

Kunihiko Yamauchi
Osaka University
81 PUBLICATIONS **2,221** CITATIONS
SEE PROFILE

Takeshi Inaoka
University of the Ryukyus
62 PUBLICATIONS **835** CITATIONS
SEE PROFILE

Tamio Oguchi
Osaka University
197 PUBLICATIONS **3,105** CITATIONS
SEE PROFILE

All content following this page was uploaded by Susumu Yanagisawa on 30 December 2014.

The user has requested enhancement of the downloaded file.

Origin of the band dispersion in a metal phthalocyanine crystal

Susumu Yanagisawa,[1,*] Kunihiko Yamauchi,[2] Takeshi Inaoka,[1] Tamio Oguchi,[2] and Ikutaro Hamada[3,†]

[1]*Department of Physics and Earth Sciences, Faculty of Science, University of the Ryukyus, 1 Senbaru, Nishihara, Okinawa 903-0213, Japan*

[2]*Institute of Scientific and Industrial Research, Osaka University, 8-1 Mihogaoka, Ibaraki, Osaka 567-0047, Japan*

[3]*International Center for Materials Nanoarchitectonics (WPI-MANA) and Global Research Center for Environment and Energy based on Nanomaterials Science (GREEN), National Institute for Materials Science, Tsukuba 305-0044, Japan*

(Received 25 September 2014; revised manuscript received 12 November 2014; published 23 December 2014; corrected 29 December 2014)

Understanding the crystal structure and electronic states of the organic semiconductor is of fundamental importance for developing the materials for the organic electronics. However, the theoretical treatment of organic semiconductors remains challenging, as the semilocal density functional theory fails to describe the dispersion forces accurately. We use van der Waals inclusive density functionals to study the zinc phthalocyanine polymorphs. It is found that the structure and energetics are well described with the van der Waals density functional, and as a result, the electronic band structure is nicely reproduced. Furthermore, we reveal that the distance between the molecules and the molecule tilt angle are important factors that determine the electronic band dispersion.

DOI: 10.1103/PhysRevB.90.245141 PACS number(s): 71.20.Rv, 71.45.Gm, 81.05.Fb

I. INTRODUCTION

Organic semiconductors have attracted enormous attention as a component of the prospective organic (opt)electronics, owing to the advantages over the prevailing inorganic semiconductor, such as low-cost fabrication processes, flexibility, and low-power consumption. Their relevant electronic properties, such as charge transport, are determined not only by the electronic structures of constituent molecules, but also by their conformation and configuration [1]. Charge carriers play crucial roles in operation of the electronic devices: They are injected into the organic semiconductors from the electrodes in the case of organic light-emitting diodes and field-effect transistors, or they are generated within the materials in the case of photovoltaic cells via photoinduced charge separation at the organic donor-acceptor interface. Understanding the crystal structure, electronic states, and their interplay is of central importance to clarify the factor determining the electronic and transport properties of organic semiconductors.

Recent progress in the experimental technique, specifically, the angle resolved photoemission spectroscopy (ARPES) enables one to measure the precise electronic band structures of organic semiconductors. As such, sexiphenyl [2], pentacene [3–5], rubrene [6], anthracene [7], and picene [8] are reported to show considerable electronic band dispersion of the width larger than 100 meV, and the bandlike carrier transport mechanism is proposed for these organic semiconductors. More recently, Yamane and Kosugi [9] have succeeded in measuring the band dispersion of metal phthalocyanine (MPc) and fluorinated MPc crystal films, which have the bandwidth of sub-100 meV, and discussed the factors determining the band dispersion of MPc crystals.

Theoretical calculations are indispensable to elucidate the mechanism of the electronic band structure [10–12] and the charge transport [13–17] for the organic semiconductors. The interaction between organic molecules is dominated by the London dispersion force, or the van der Waals (vdW) force, which is poorly described by the semilocal density functional theory (DFT), hindering the theoretical treatment of the organic semiconductors. However, it is becoming possible to describe the structure and energetics of organic crystals very accurately, thanks to the recent advances in the method for the dispersion interactions [18–25].

In this article we have investigated the atomic and electronic structures of the zinc phthalocyanine (ZnPc) crystal, by using a recent version [24] of the van der Waals density functional (vdW-DF) [28] to elucidate the mechanism of the band dispersion for the ZnPc crystal, one of key materials for organic photoelectronic devices [29–31].

II. METHOD

The calculations were performed using the projector augmented wave method [32] as implemented in the Vienna *ab initio* simulation package [33,34]. The vdW-DF calculations were done using the efficient algorithm of Román-Pérez and Soler [35], implemented by Klimeš *et al.* [36]. We used rev-vdW-DF2 [24], which employs a revised Becke's exchange [37] and the nonlocal correlation of vdW-DF2 [38]. The rev-vdW-DF2 has been shown to predict the structure and binding energy of organic crystals accurately [24]. The wave functions were expanded in terms of a plane wave basis set with a cutoff energy of 756 eV. In this work we considered ZnPc in the α-CuPc structure (α-ZnPc) [26] as suggested in the previous work [9], as well as β-ZnPc [27] (Fig. 1). The α and γ forms are found in ZnPc thin film [39], but the latter is not considered here, as the detailed crystal structure is not known. The Brillouin zone integration was performed using a $2 \times 6 \times 2$ k-point set for both structures. The equilibrium volume was determined by fitting the calculated total energy as a function of volume to the Birch-Murnaghan equation of states. At each volume, cell parameters, as well as the internal degree of freedom, were fully relaxed until the forces acting on atoms become less than 5×10^{-3} eV Å^{-1}. Binding energy was evaluated by subtracting the total energy of the isolated ZnPc molecule(s) from the total energy of the ZnPc crystal at the equilibrium. Zero-point vibration energy was not taken into account.

*shou@sci.u-ryukyu.ac.jp

†Author to whom correspondence should be addressed: HAMADA.Ikutaro@nims.go.jp

 ©2014 American Physical Society

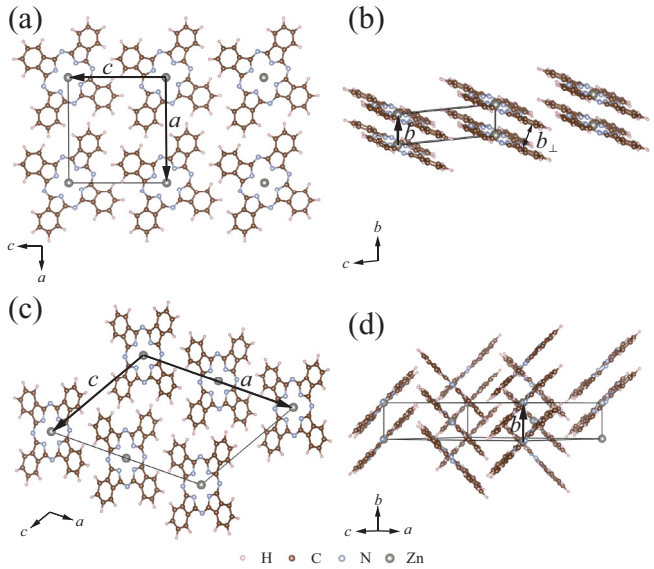

FIG. 1. (Color online) Crystal structures of the ZnPc polymorphs. Projection onto (a) [010] plane and (b) [100] plane of α-ZnPc. Projection onto (c) [010] plane and (d) [110] plane of β-ZnPc.

III. RESULTS AND DISCUSSION

α-ZnPc belongs to the space group of $P\bar{1}$ (triclinic), containing one molecule per unit cell, and β-ZnPc has the monoclinic cell with the space group of $P2_1/a$ (two molecules per unit cell). The detailed crystal structure has been reported only for the β-ZnPc [27]. However, it has been suggested that the structures and properties of α-CuPc and α-ZnPc are similar [40], and thus the crystal structure of α-CuPc [26] was used as an initial guess for the α-ZnPc. Optimized cell parameters and binding energy at the equilibrium are summarized in Table I. The lattice parameters for α-ZnPc obtained with rev-vdW-DF2 are in good agreement with those for α-CuPc, while the Perdew-Burke-Ernzerhof (PBE) [41] generalized gradient approximation severely overestimates (underestimates) lattice parameters (binding energy), suggesting the importance of the dispersion force in the ZnPc crystal. We calculated the molecular tilt angle, defined as the angle between the vector normal to the molecular plane and the lattice vector $\boldsymbol{b}$, and the intermolecular distance along the direction normal to the molecular plane [$b_\perp$, see Fig. 1(b)] to obtain 27.8° and 3.30 Å, respectively. The calculated intermolecular distance ($b_\perp$) is in reasonable agreement with the experimental estimate of 3.326 Å [9], considering the facts that the molecule is flat-lying on the substrate with the tilt angle of 0°–5° and that the orientation of molecules with respect to the lattice vector $\boldsymbol{b}$ is not known in the experiment. For α-ZnPc, we also used other functionals, including vdW-DF2 [38], optB88-vdW [42], optB86b-vdW [36], vdW-DF^{C09_x} [43], vdW-DF2^{C09_x} [44], and semiempirical DFT-D2 [45] for comparison. It is found that vdW-DF2 tends to predict larger lattice parameters, and the others predict smaller lattice parameters. Consequently, vdW-DF2 predicts smaller binding energy, and the others (except for vdW-DF2^{C09_x}) give larger energy [46].

In the case of β-ZnPc, optimized lattice parameters with rev-vdW-DF2 are in excellent agreement with the experiment (within the error of 0.4%), implying that the structure for α-ZnPc is also predicted accurately. By calculating the binding energy, we find that β-ZnPc is more stable than α-ZnPc, consistent with the experimental suggestion that the β phase is the stable structure, while α is a metastable one [47]. In the following we discuss the electronic band structure for the α-ZnPc, as it is the suggested [9] structure in the ZnPc crystal film.

In the ARPES experiment [9], the band structure of α-ZnPc was obtained by assuming that there are two molecules per unit cell, the setting similar to the one used in Ref. [48]. To enable direct comparison with the experiment, we doubled the optimized unit cell of α-ZnPc in the $\boldsymbol{b}$ direction for the band structure calculations. The calculated band structure of α-ZnPc is displayed in Fig. 2 (see Supplemental Material Fig. S1 [46] for the band structures with other vdW-DFs). The valence and conduction bands originate from the C $2p$ orbitals, which constitute the highest occupied molecular orbitals (HOMO) and the doubly degenerated lowest unoccupied molecular orbitals (LUMO) of the gas-phase ZnPc molecule, respectively. The second HOMO (HOMO–1) derived band is comprised of the $3d$ states of the central Zn atom. This assignment is consistent with that for a gas-phase ZnPc molecule within semilocal DFT [49]. The valence (HOMO) band has a dispersion with the width of 64 meV along the Γ-Y direction [50], and almost no dispersion is found for the other directions. The LUMO derived-conduction band has the larger dispersion along the Γ-Y direction. The

TABLE I. Optimized lattice parameters (a, b, c, α, β, and γ), equilibrium unit cell volume (V_0), and binding energy E_b for ZnPc in the α- and β-polymorphs, along with the experimental values.

	a (Å)	b (Å)	c (Å)	α (deg)	β (deg)	γ (deg)	V_0 (Å^3)	E_b (eV/mol)
				α-ZnPc				
PBE	13.927	4.486	13.305	100.11	91.00	89.17	817.99	–0.16
rev-vdW-DF2	12.902	3.731	12.026	95.19	90.06	91.02	576.42	–2.43
Expt. (α-CuPc)[a]	12.886	3.769	12.061	96.22	90.62	90.32	582.27	
				β-ZnPc				
rev-vdW-DF2	19.204	4.836	14.517	90.0	120.49	90.0	1161.67	–2.95
Expt.[b]	19.274 (5)	4.8538 (15)	14.553 (4)	90.0	120.48 (2)	90.0	1173.32	

[a]Reference [26].
[b]Reference [27].

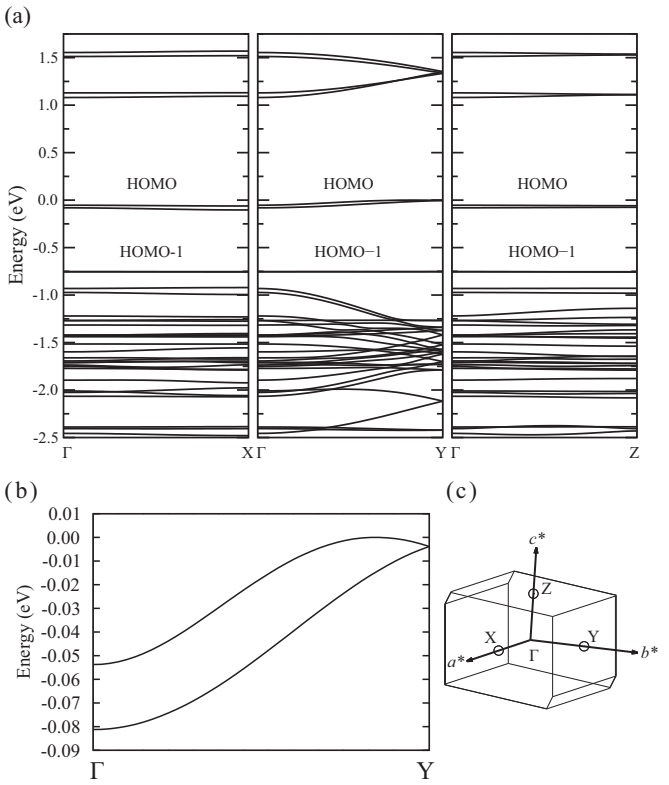

FIG. 2. (a) Electronic band structure for α-ZnPc. (b) Magnified HOMO band along the Γ-Y direction. The origin of the energy is set to the valence band maximum. (c) Brillouin zone for the α-ZnPc. $\Gamma = (0,0,0)$, $X = (1/2,0,0)$, $Y = (0,1/2,0)$, and $Z = (0,0,1/2)$ in the unit of reciprocal lattice vectors.

bandwidth for the HOMO band is slightly smaller than the experimental value of 92 meV [9], but the agreement is fairly nice. We performed the band structure calculation with the Heyd-Scuseria-Ernzerhof (HSE) [51] hybrid functional at the rev-vdW-DF2 optimized structure, and found that the bandwidth obtained with HSE is almost the same (67 meV). We also performed the one-shot G_0W_0 calculations using the GW space-time code [52–54] with the PBE orbitals [55] and the norm conserving pseudopotentials [56], to obtain the larger bandwidth of 77 meV than the PBE value of 59 meV. The result is in line with the previous work on the rubrene crystal, where the larger bandwidth is obtained with the G_0W_0 approximation [57]. We also note that a discrepancy is found for the HOMO–1 band and the band below it (π band): Experimentally, the HOMO–1 band is located $\sim$1 eV above the π band, and has a considerable band dispersion. However, the calculated width for the HOMO–1 band is very small and it is close to the π band. We presume this is because the energy level for HOMO–1 is too shallow with the semilocal DFT as shown in Ref. [58], and the error is also mitigated by the use of the G_0W_0 approximation with an appropriate treatment of the semicore states. For the discussion on the HOMO band dispersion, however, the semilocal level of approximation is sufficient, and the conclusion is unchanged when the highly accurate electronic structure method is used as discussed above.

By inspecting the wave functions for the HOMO band in real space, we found that there is no appreciable overlap between molecular orbitals in the neighboring molecules, in contrast to what have been found in other organic solid such as rubrene [57].

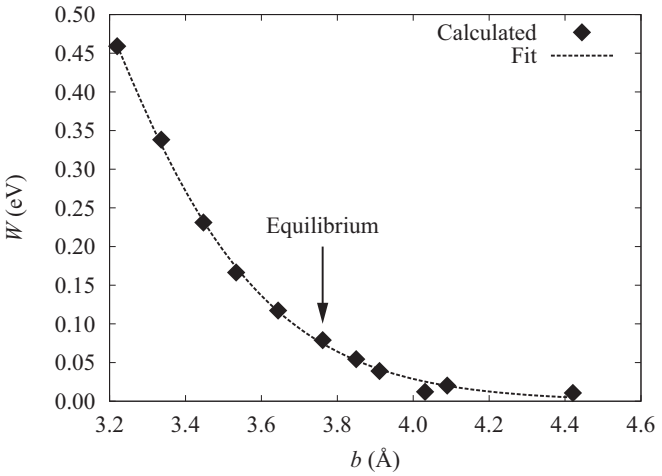

FIG. 3. Bandwidth (W) for α-ZnPc as a function of lattice parameter b. The W is defined as the difference between the energy levels for the top and the bottom of the valence band along the Γ-Y direction.

Figure 3 depicts the bandwidth (W) as a function of lattice constant b (π-stacking direction), which were obtained by performing band structure calculations using the fully relaxed

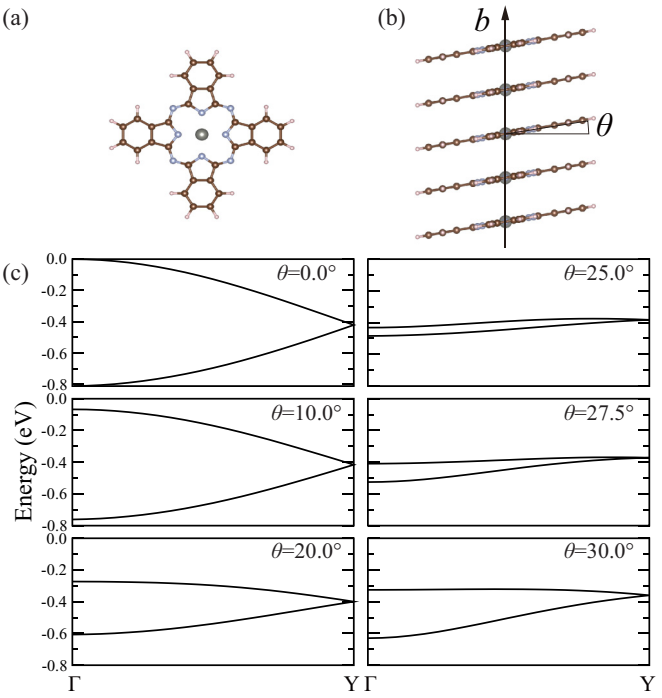

FIG. 4. (Color online) Top view (a) and side view (b) of the hypothetical quasi-one-dimensional chain of ZnPc. Lattice constant along the molecular stacking direction (b) is set to 3.731 Å and the lateral dimension is 22.5 × 22.5 Å^2. (c) Band structure along the molecular stacking direction as a function of the tilt angle θ. The origin of the energy is set to the valence band top at $\theta = 0°$. The Y point corresponds to the Brillouin zone edge for the supercell containing two ZnPc molecules.

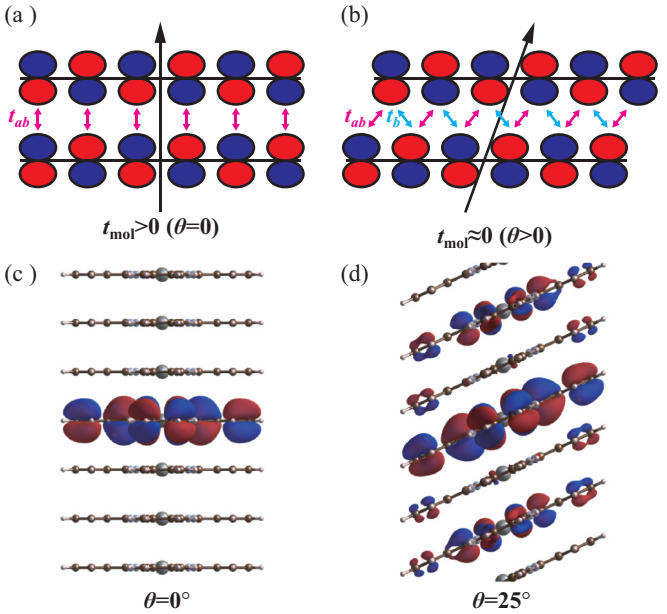

FIG. 5. (Color online) Schematic illustration of the transfer integral between the molecules (t_{mol}) in the case of the molecular tilt angle $\theta = 0^\circ$ (a) and $\theta > 0^\circ$ (b). t_{ab} and t_b indicate the antibonding and bonding type components of the transfer integral, respectively. t_{mol} indicates the total transfer integral between the molecules. The maximally localized Wannier function at $\theta = 0^\circ$ (c) and $\theta = 25^\circ$ (d). The former is localized on one molecule, and the latter mainly on one molecule and partially on the next nearest molecules.

structures at different volumes (see Fig. S2 [46]). Here the W is defined by the difference between the calculated energy levels of top and bottom of the valence band. The W is nicely fitted to a function $W(b) = \sum_{i=0}^{4} c_i b^i e^{-db}$, where $\{c_i\}$ and d are fitting parameters, and thus, we suggest that the linear relationship proposed in Ref. [9] holds only in a small region of the intermolecular distance. We also calculated W as a function of b (i) by varying the cell parameter b while other degrees of freedom are fixed and (ii) by varying all the cell lengths (a, b, and c) at the same ratio with the internal molecular geometry fixed to the equilibrium one, and found that similar behavior of W (Fig. S3 [46]), suggesting that the distance between the molecules in the π-stacking direction is the important factor determining the band dispersion. This is in line with the result by Brédas *et al.* [59], who have shown that the electronic

TABLE II. Transfer integrals for the nearest neighbor (t_1) and for the next nearest neighbor (t_2) in the quasi-one-dimensional ZnPc chain calculated based on the maximally localized Wannier function.

Angle (deg)	t_1 (meV)	t_2 (meV)
0.0	202	6
10.0	174	2
20.0	85	–10
25.0	16	–19
27.5	–25	–25
30.0	–70	–32

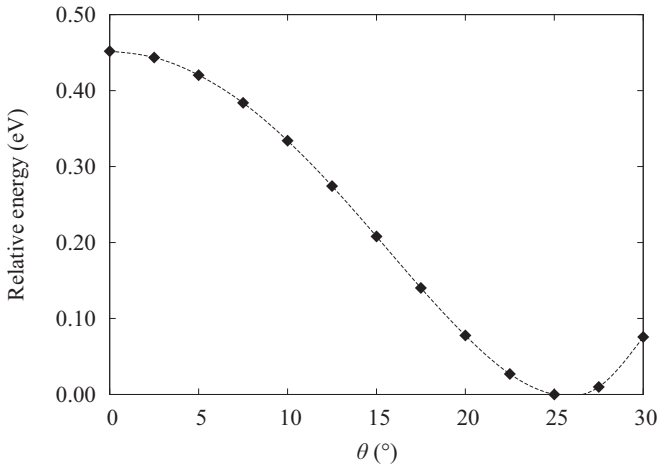

FIG. 6. Total energy of a quasi-one-dimensional ZnPc chain as a function of the tilt angle θ. The energy origin is set to the one at the angle of 25°. The line is the guide for the eyes. See Fig. 4 for the molecular geometry.

splitting (bandwidth) decreases exponentially as the distance between molecules increases.

To gain more insight into the mechanism of the band dispersion, we investigated the role of the molecular tilt by constructing a quasi-one-dimensional chain with one ZnPc molecule per unit cell [Figs. 4(a) and 4(b)] and calculated the band structure along the chain direction. In Fig. 4(c) we plot the HOMO band as a function of the molecular tilt angle θ ($0^\circ \leqslant \theta \leqslant 30^\circ$). The band is folded to compare directly with that in Fig. 2. The band dispersion follows a (folded) simple tight-binding model, i.e., $\epsilon(k) = \epsilon_0 + 2t_1 \cos(kb) + 2t_2 \cos(2kb)$ with a p type orbital, where k is the wave vector, ϵ_0 is the on-site energy, t_1 and t_2 are the transfer integral for the nearest neighbor and the second nearest neighbor, respectively, and b is the lattice constant along the molecular

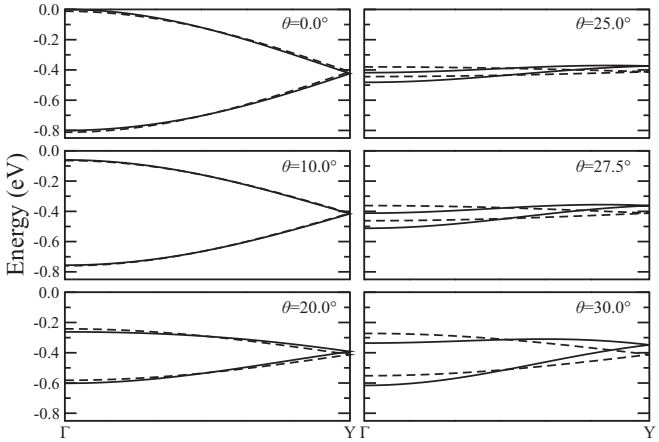

FIG. 7. Tight-binding band structure for the hypothetical quasi-one-dimensional ZnPc chain along the molecular stacking direction as a function of the tilt angle θ, using the transfer integrals for the nearest neighbor (t_1) and the next nearest neighbor (t_2) (solid line), and that with t_1 only (dashed line). See Fig. 4 for the molecular geometry.

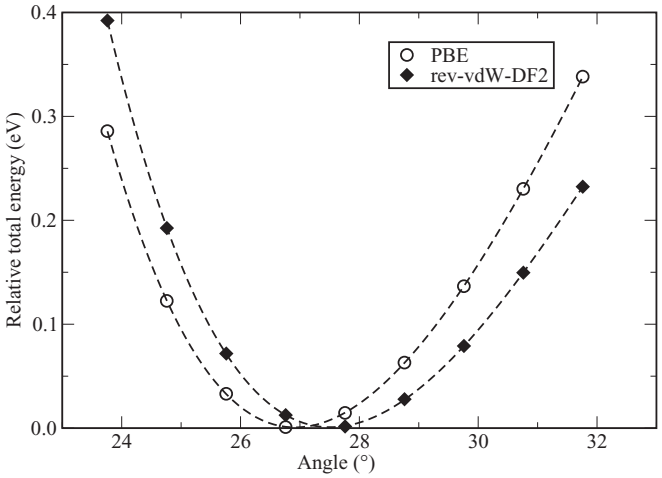

FIG. 8. Total energy of α-ZnPc as a function of molecular tilt angle defined as the angle between the vector normal to the ZnPc molecule plane and the lattice vector **b**. For comparison, the PBE total energy is also plotted. The line is the guide for the eyes. The equilibrium angle obtained with PBE is slightly different from that with rev-vdW-DF2, because the rev-vdW-DF2 geometry was used in the PBE calculations. The molecular plane is defined by the vectors connecting Zn and surrounding N atoms, which form a flat surface, as the ZnPc molecule is slightly distorted in the crystal. The energy zero is set to that at the minimum obtained using each density functional.

stacking direction. At $\theta = 0^\circ$, where $|t_1| \gg |t_2|$, the bonding and antibonding states are clearly seen. This band structure is far from the experimental and calculated ones for α-ZnPc. However, at $20^\circ \leqslant \theta \leqslant 30^\circ$, the phase of the molecular orbital is modulated considerably because of the molecular tilt, resulting in a small bandwidth and the valence band maximum near the Y point. At $\theta = 25^\circ$, bandwidth takes the minimum value of 82 meV, in good correspondence to the theoretical bandwidth of 68 meV at the tilt angle of 27.8° for α-ZnPc.

To explain this angle dependence, we illustrate the transfer integrals between the molecules for $\theta = 0$ and $\theta > 0$ in Figs. 5(a) and 5(b), respectively. When θ is small, antibonding type interaction is dominant in the transfer integral. However, as θ increases, the bonding type interaction gets larger and compensates for the antibonding type components, resulting in a small $|t_1|$ and bandwidth, and gain in the band energy. Indeed, the calculated transfer integral t_1 based on the maximally localized Wannier function [MLWF, Figs. 5(c) and 5(d)] [60,61] is found to decrease as θ increases (Table II), and the total energy of this hypothetical ZnPc chain takes the minimum at $\theta = 25^\circ$ (Fig. 6). The mechanism is essentially the same as the one discussed by Brédas *et al.* [59], where the molecular coupling varies depending on the relative displacement in a molecular dimer. Since t_1 decreases as θ increases, here we also consider the transfer integral for the next nearest neighbor t_2, leading to an additional term $2t_2 \cos(2kb)$ in $\epsilon(k)$. It is found that the magnitude of t_2 increases as θ increases. Near the equilibrium, $|t_2|$ becomes comparable to $|t_1|$, which results in the modulation of the HOMO band dispersion. This result indicates the importance of t_2 in determining the band structure. A one-dimensional tight-binding model with t_1 and t_2 based on MLWF nicely reproduces the DFT band structure, whereas the tight-binding model with t_1 only provides less satisfactory results near the equilibrium (Fig. 7), supporting our findings described above. We also calculated the transfer integral for α-ZnPc to obtain $t_1 = 9$ meV and $t_2 = -17$ meV, in good agreement with those calculated for the hypothetical ZnPc chain. Finally, we calculated the total energy of α-ZnPc as a function of molecular tilt angle and found that the total energy has the minimum at its equilibrium angle with insignificant effect of the dispersion force, suggesting that the molecular tilt is determined so as to minimize the band energy (Fig. 8). Taken together, these results demonstrate the critical role of the molecular tilt in determining the band dispersion as well as the structural stability.

IV. CONCLUSION

We have studied the atomic and electronic structures of the ZnPc crystal with vdW-DF (rev-vdW-DF2). It is found that the vdW forces are essential to describe the crystal structure accurately, and using the optimized structure, the electronic band structure of ZnPc is nicely reproduced. We reveal that the distance between the molecules and the tilt angle between the lattice vector and the molecular plane are important factors that determine the band dispersion. Accurate and precise vdW inclusive electronic structure calculations will help to understand/develop materials for organic electronics.

ACKNOWLEDGMENTS

We thank Masayuki Toyoda for fruitful discussion. This work was partly supported by the Grants-in-Aid for Scientific Research (C) (No. 22540332), for Young Scientists (B) (No. 26810009), and for Scientific Research on Innovative Areas "3D Active-Site Science" (No. 26105011) from Japan Society for the Promotion of Science, by Cooperative Research Program of Network Joint Research Center for Materials and Devices in ISIR, Osaka University, by World Premier International Research Center Initiative (WPI), Ministry of Education, Culture, Sports, Science and Technology (MEXT) in Japan, and by MEXT Program for Development of Environmental Technology using Nanotechnology. We acknowledge the Supercomputer Center, the Institute for Solid State Physics, the University of Tokyo, and the Cyberscience Center, Tohoku University, for the use of their facilities. The molecular graphics were generated with VESTA [62].

[1] V. Coropceanu, J. Cornil, D. A. da Silva Filho, Y. Olivier, R. Silbey, and J.-L. Brédas, Chem. Rev. **107**, 926 (2007).

[2] G. Koller, S. Berkebile, M. Oehzelt, P. Puschnig, C. Ambrosch-Draxl, F. P. Netzer, and M. G. Ramsey, Science **317**, 351 (2007).

[3] H. Kakuta, T. Hirahara, I. Matsuda, T. Nagao, S. Hasegawa, N. Ueno, and K. Sakamoto, Phys. Rev. Lett. **98**, 247601 (2007).

[4] S. Berkebile, P. Puschnig, G. Koller, M. Oehzelt, F. P. Netzer, C. Ambrosch-Draxl, and M. G. Ramsey, Phys. Rev B **77**, 115312 (2008).

[5] S. Ciuchi, R. C. Hatch, H. Höchst, C. Faber, X. Blase, and S. Fratini, Phys. Rev. Lett. **108**, 256401 (2012).
[6] S.-I. Machida, Y. Nakayama, S. Duhm, Q. Xin, A. Funakoshi, N. Ogawa, S. Kera, N. Ueno, and H. Ishii, Phys. Rev. Lett. **104**, 156401 (2010).
[7] F. Bussolotti, Y. Yamada-Takamura, Y. Wang, and R. Friedlein, J. Chem. Phys. **135**, 124709 (2011).
[8] Q. Xin, S. Duhm, F. Bussolotti, K. Akaike, Y. Kubozono, H. Aoki, T. Kosugi, S. Kera, and N. Ueno, Phys. Rev. Lett. **108**, 226401 (2012).
[9] H. Yamane and N. Kosugi, Phys. Rev. Lett. **111**, 086602 (2013).
[10] P. Puschnig and C. Ambrosch-Draxl, Phys. Rev. B **60**, 7891 (1999).
[11] P. Puschnig, K. Hummer and C. Ambrosch-Draxl, G. Heimel, M. Oehzelt, and R. Resel, Phys. Rev. B **67**, 235321 (2003).
[12] K. Hummer and C. Ambrosch-Draxl, Phys. Rev. B **72**, 205205 (2005).
[13] A. Troisi and G. Orlandi, Phys. Rev. Lett. **96**, 086601 (2006).
[14] A. Troisi, Chem. Soc. Rev. **40**, 2347 (2011).
[15] H. Tamura, M. Tsukada, H. Ishii, N. Kobayashi, and K. Hirose, Phys. Rev. B **86**, 035208 (2012).
[16] H. Ishii, K. Honma, N. Kobayashi, and K. Hirose, Phys. Rev B **85**, 245206 (2012).
[17] C. Motta and S. Sanvito, J. Chem. Theor. Comput. **10**, 4624 (2014).
[18] J. Kleis, B. I. Lundqvist, D. C. Langreth, and E. Schröder, Phys. Rev. B **76**, 100201(R) (2007).
[19] D. Lu, Y. Li, D. Rocca, and G. Galli, Phys. Rev. Lett. **102**, 206411 (2009).
[20] A. Tkatchenko and M. Scheffler, Phys. Rev. Lett. **102**, 073005 (2009).
[21] A. Otero-de-la-Roza and E. R. Johnson, J. Chem. Phys. **136**, 174109 (2012); **137**, 054103 (2012).
[22] A. Tkatchenko, R. A. DiStasio, Jr., R. Car, and M. Scheffler, Phys. Rev. Lett. **108**, 236402 (2012).
[23] J. Klimeš and A. Michaelides, J. Chem. Phys. **137**, 120901 (2012), and references therein.
[24] I. Hamada, Phys. Rev. B **89**, 121103(R) (2014).
[25] A. M. Reilly and A. Tkatchenko, Phys. Rev. Lett. **113**, 055701 (2014).
[26] A. Hoshino, Y. Takenaka, and H. Miyaji, Acta Crystallogr. Sect. B: Struct. Sci. **59**, 393 (2003).
[27] W. R. Scheidt and W. Dow, J. Am. Chem. Soc. **99**, 1101 (1977).
[28] M. Dion, H. Rydberg, E. Schröder, D. C. Langreth, and B. I. Lundqvist, Phys. Rev. Lett. **92**, 246401 (2004).
[29] C. C. Lenzoff and A. B. P. Lever, Eds., *Phthalocyanines, Properties and Applications* (VCH, New York, 1989-1996), Vols. 1–4.
[30] N. B. Mckeown, *Phthalocyanine Materials* (Cambridge University Press, Cambridge, 1998).
[31] D. Wöhrle and D. Meissner, Adv. Mater. **3**, 129 (1991).
[32] P. E. Blöchl, Phys. Rev. B **50**, 17953 (1994).
[33] G. Kresse and J. Furthmüller, Phys. Rev. B **54**, 11169 (1996).
[34] G. Kresse and D. Joubert, Phys. Rev. B **59**, 1758 (1999).
[35] G. Román-Pérez and J. M. Soler, Phys. Rev. Lett. **103**, 096102 (2009).
[36] J. Klimeš, D. R. Bowler, and A. Michaelides, Phys. Rev. B **83**, 195131 (2011).
[37] A. D. Becke, J. Chem. Phys. **85**, 7184 (1986).
[38] K. Lee, É. D. Murray, L. Kong, B. I. Lundqvist, and D. C. Langreth, Phys. Rev. B **82**, 081101(R) (2010).
[39] F. Iwatsu, J. Crystal Growth **71**, 629 (1985).
[40] C. Schünemann, C. Elschner, A. A. Levin, M. Levichkova, K. Leo, and M. Riede, Thin Solid Films **519**, 3939 (2011).
[41] J. P. Perdew, K. Burke, and M. Ernzerhof, Phys. Rev. Lett. **77**, 3865 (1996).
[42] J. Klimeš, D. R. Bowler, and A. Michaelides, J. Phys.: Condens. Matter **22**, 022201 (2010).
[43] V. R. Cooper, Phys. Rev. B **81**, 161104(R) (2010).
[44] I. Hamada and M. Otani, Phys. Rev. B **82**, 153412 (2010).
[45] S. Grimme, J. Comput. Chem. **27**, 1787 (2006).
[46] See Supplemental Material at http://link.aps.org/supplemental/10.1103/PhysRevB.90.245141 for additional information.
[47] F. Iwatsu, T. Kobayashi, and N. Uyeda, J. Phys. Chem. **84**, 3223 (1980).
[48] G. Giovannetti, G. Brocks, and J. van den Brink, Phys. Rev B **77**, 035133 (2008).
[49] M.-S. Liao and S. Scheiner, J. Chem. Phys. **114**, 9780 (2001).
[50] To make a comparison with the experiment [9], the bandwidth of the HOMO band was calculated from the difference between the energy level at the Y point and the midpoint of the energy levels at the Γ point. See Fig. 1(a) of Ref. [9]. The bandwidth calculated from the bottom and top of the HOMO band is 81 meV.
[51] J. Heyd, G. E. Scuseria, and M. Ernzerhof, J. Chem. Phys. **118**, 8207 (2003).
[52] M. M. Rieger, L. Steinbeck, I. D. White, H. N. Rojas, and R. W. Godby, Comput. Phys. Commun. **117**, 211 (1999).
[53] L. Steinbeck, A. Rubio, L. Reining, M. Torrent, I. D. White, and R. W. Godby, Comput. Phys. Commun. **125**, 105 (2000).
[54] C. Freysoldt, P. Eggert, P. Rinke, A. Schindlmayr, R. W. Godby, and M. Scheffler, Comput. Phys. Commun. **176**, 1 (2007).
[55] Y. Morikawa, H. Ishii, and K. Seki, Phys. Rev. B **69**, 041403 (2004).
[56] N. Troullier and J. L. Martins, Phys. Rev. B **43**, 1993 (1991).
[57] S. Yanagisawa, Y. Morikawa, and A. Schindlmayr, Phys. Rev. B **88**, 115438 (2013).
[58] P. Umari and S. Fabris, J. Chem. Phys. **136**, 174310 (2012).
[59] J.-L. Brédas, J. P. Calbert, D. A. da Silva Filho, and J. Cornil, Proc. Natl. Acad. Sci. USA **99**, 5804 (2002).
[60] N. Marzari, A. A. Mostofi, J. R. Yates, I. Souza, and D. Vanderbilt, Rev. Mod. Phys. **84**, 1419 (2012).
[61] A. A. Mostofi, J. R. Yates, Y.-S. Lee, I. Souza, D. Vanderbilt, and N. Marzari, Comput. Phys. Commun. **178**, 685 (2008).
[62] K. Momma and F. Izumi, J. Appl. Crystallogr. **44**, 1272 (2011).

View publication stats